Experimental Eye Research 209 (2021) 108681

Contents lists available at ScienceDirect

Experimental Eye Research

journal homepage: www.elsevier.com/locate/yexer

# Distribution of planar cell polarity proteins in the developing avian retina

Guadalupe Álvarez-Hernán [a], Sergio Garrido-Jiménez [b], Ángel Carlos Román [b], José María Carvajal-González [b,**], Javier Francisco-Morcillo [a,*]

[a] Área de Biología Celular, Departamento de Anatomía, Biología Celular y Zoología, Facultad de Ciencias, Universidad de Extremadura, Badajoz, Spain
[b] Departamento de Bioquímica, Biología Molecular y Genética, Facultad de Ciencias, Universidad de Extremadura, Badajoz, Spain

ARTICLE INFO

*Keywords:*
Axonal guidance
Cell asymmetry
Cell morphogenesis
Development
Retinogenesis
Planar cell polarity

ABSTRACT

Planar cell polarity (PCP) is evolutionary conserved and play a critical role in proper tissue development and function. During central nervous system development, PCP proteins exhibit specific patterns of distribution and are indispensable for axonal growth, dendritogenesis, neuronal migration, and neuronal differentiation. The retina constitutes an excellent model in which to study molecular mechanisms involved in neural development. The analysis of the spatiotemporal expression of PCP proteins in this model constitutes an useful histological approach in order to identify possible roles of these proteins in retinogenesis. Immunohistochemical techniques revealed that Frz6, Celsr1, Vangl1, Pk1, Pk3, and Fat1 were present in emerging axons from recently differentiated ganglion cells in the chicken retina. Except for Vangl1, they were also asymmetrically distributed in differentiated amacrine cells. Pk1 and Pk3 were restricted in the outer nuclear layer to the outer segment of photoreceptors. Vangl1 was also located in the cell somata of Müller glia. Given these findings together, the distribution of PCP proteins in the developing chicken retina suggest essential roles in axonal guidance during early retinogenesis and a possible involvement in the establishment of cell asymmetry and maintenance of retinal cell phenotypes.

## 1. Introduction

Planar cell polarity (PCP) consists in a coordinate alignment of cells across a tissue plane. Initial and important studies have been carried out in the wing of *Drosophila melanogaster* to establish the features and function of the proteins involved in it, in both adult and developing tissues (Das et al., 2002; Bastock et al., 2003). All these developmental events are regulated by two different pathways: the Fat-Dachsous (Ft-Ds) group and the Frizzled-PCP core (Fz-PCP) (Singh and Mlodzik, 2012; Devenport, 2014). The first one is commanded by the interaction of the extracellular domains of the protocadherins Fat (Fat) and Dachsous (Ds) that are located at the plasma membrane of neighbour cells and by a Golgi's transmembrane kinase named Four-Jointed (Fj) that regulates this extracellular interaction between Ft and Ds (Devenport, 2014). On the other hand, Fz-PCP is constituted by transmembrane proteins like Frizzled (Fz, Fzd1-10 in vertebrates), Van Gogh/Strabismus (Vang/Stbm, Vangl1 and Vangl2 in vertebrates) and Flamingo (Fmi, also known as Celsr1-3 in vertebrates) and by cytoplasmatic proteins like Dishevelled (Dsh, Dvl1-3 in vertebrates), Prickle (Pk) and Diego (Dgo).

Components of both pathways are functionally conserved in vertebrates and are also involved in essential morphogenetic processes during embryonic development, for example appropriate limb development direction (Gao et al., 2018) or to support spermatogenesis (Li et al., 2020) (for reviews, see Goodrich and Strutt, 2011; Butler and Wallingford, 2017). At very early stages of development, PCP signaling controls the establishment of left-right asymmetry (Axelrod, 2020).

The core PCP genes also plays an essential role in the development and function of the central nervous system (CNS). Indeed, it has been described that most of the PCP components are thoroughly expressed and play a fundamental role in CNS organogenesis (Tissir and Goffinet, 2010), neural tube closure (Butler and Wallingford, 2018), and axonal outgrowth and guidance and synapse formation (Zou, 2020). Related to sense systems, the majority of the studies have been carried out in the inner ear (Duncan et al., 2017; Najarro et al., 2020), pointing that some PCP components are crucial proteins for the correct orientation of the hair cells. Given its well-known and highly ordered structure, the neural

* Corresponding author. Área de Biología Celular, Departamento de Anatomía, Biología Celular y Zoología, Facultad de Ciencias, Universidad de Extremadura, 06006, Badajoz, Spain.
** Corresponding author. Departamento de Bioquímica y Biología Molecular y Genética, Facultad de Ciencias, Universidad de Extremadura. 06006, Badajoz, Spain.
*E-mail addresses:* jmcarvaj@unex.es (J.M. Carvajal-González), morcillo@unex.es (J. Francisco-Morcillo).

https://doi.org/10.1016/j.exer.2021.108681
Received 24 February 2021; Received in revised form 3 June 2021; Accepted 17 June 2021
Available online 21 June 2021

retina also offers an ideal model to study the possible role of PCP proteins in the mechanisms involved in assembling neural synapses and cell morphology. *Fzd* genes are expressed in different embryo tissues during early stages of development including the eyes (Fuhrmann et al., 2003; Seigfried et al., 2017; Onishi et al., 2020). In the case of the retina, *Fzd3* is required for retinal axon guidance (Hua et al., 2014) and is also involved in morphological maturation of bipolar cells, and in the establishment of synapses between rods and bipolar cells (Shen et al., 2016). Little is known about Celsr proteins distribution in the eye tissues. It has been described that Celsr3 is involved in the differentiation process of a subset of inhibitory amacrine and bipolar cells in the zebrafish retina (Lewis et al., 2011, 2015). The expression and function of Vangl1 during eye development remain unexplored, but it has been described that *Vangl2* is essential for the establishment of the ganglion cell axon correct trajectories (Rachel et al., 2000; Torban et al., 2007). Mutations on *Prickle* genes lead to defects in photoreceptor maturation (Liu et al., 2013), abnormal neurite growth of subtypes of retinal cells (Mei et al., 2014), and severe retinal deficiencies (Yu et al., 2020). Fat-like cadherins are required for morphogenesis of eye rudiment. The deletion of some of the members of the Fat-genes leads to ocular defects in mouse and zebrafish (Ciani et al., 2003; Sugiyama et al., 2016; Lahrouchi et al., 2019). These proteins also regulate angiogenesis and astrocyte maturation in the vertebrate retina (Caruso et al., 2013; Helmbacher, 2020). Fat-cadherins also guide cell migration *in vivo* during mouse retinal development (Deans et al., 2011) and are involved in lens epithelial cell polarity (Sugiyama et al., 2016).

In addition to these functional studies about the implication of PCP proteins during visual system development in vertebrates, little is known about the distribution of PCP components in the developing retina (Van Raay and Vetter, 2004). In fact, a comprehensive study of the expression of multiple proteins throughout all stages of retinal development in a single avian species is missing to date.

Birds are a reliable developmental model in retinal research. Among key features of this developmental system, they have large eyes and ready availability of embryos, and also detailed events of histogenesis and cell differentiation have been largely described (Prada et al., 1991; Morino et al., 1996; Drenhaus et al., 2003, 2004; Francisco-Morcillo et al., 2005; da Costa-Calaza and Gardino, 2010; Álvarez-Hernán et al., 2018, 2020; 2021; de Mera-Rodríguez et al., 2019). In this report, we investigated the distribution of several PCP proteins in the developing retina of the chicken (*Gallus,* Linnaeus 1758). Our results show that most of the proteins studied are detected in the chicken developing retina in overlapping patterns, suggesting an essential role for axonal guidance during early retinogenesis.

## 2. Material and methods

### 2.1. Animals and tissue processing

All animals were treated according to the regulations of the European Union 130 (EU Directive, 2010/63/EU) and Spain (Royal Decree 53/2013). A total of 30 White Leghorn (*G. gallus)* embryos were used in the present study (Table 1). The eggs were incubated in a rotating egg incubator (Masalles S.A.) at 37.5 °C and 80–90% humidity. Chick embryos were harvested at various times (Table 1). They were fixed with paraformaldehyde (PFA) 4% in phosphate-buffered solution (PBS) (0.1 M, pH 7.4) overnight at 4°C. For immunohistochemical analysis, samples were rinsed in PBS and then cryoprotected with PBS-Sucrose (15%) overnight at 4 °C, soaked in embedding medium, frozen onto sectioning blocks and store at −80 °C. Cryostat sections (20 μm thick) were cut in frontal plan. Sections were thaw mounted on Superfrost® Plus slides (Menzel-Glässer, Germany), air dried and stored at −20 °C.

**Table 1**
Stages and number of embryos of G. gallus used in the present study.

| Stages | N | Incubation time |
|---|---|---|
| E3 (HH19) | 10 | 68–75 h |
| E6 (HH29) | 8 | 144 h |
| E8 (HH34) | 6 | 192 h |
| E15 (HH41) | 6 | 360 h |

### 2.2. Immunohistochemistry

Working dilutions and sources of primary and secondary antibodies used in the present study are summarized in Table 2. Antigen retrieval was done by soaking the sections for 30 min in 90 °C citrate buffer, cooled to room temperature, and washed several times in 0.1% Triton-X-100 in PBS (PBS-T) and then pre-blocked in 0.2% gelatin, 0.25% Triton-X-100, Lys 0.1 M in PBS (PBS-G-T-L) for 1 h. Sections were incubated with the primary antibody in a humidified chamber at RT overnight. Then, slides were washed twice in PBS-T and in PBS-G-T and then incubated with the secondary antibody for 2 h at RT in a humidified chamber. Then, sections were washed two times in PBS-T in darkness and incubated with DAPI (4',6-diamidino-2-phenylindole) for 10 min at room temperature followed by two washes in PBS in darkness. Finally, slides were mounted with Mowiol (polyvinyl alcohol 40–88, Fluka, Ref. 81,386).

### 2.3. Image acquisition and processing

Immunolabeled sections of *G. gallus* embryos were observed using an epifluorescence, bright field Nikon Eclipse 80i microscope and photographed using an ultra-high-definition Nikon digital camera DXM1200F. Graphical enhancement and preparation for publication were performed in Adobe Photoshop (v-CS4).

**Table 2**
Immunoreagents, working dilutions, and sources of primary and secondary antibodies used in the present study.

| Primary antibody | Working dilution | Antibodies suppliers |
|---|---|---|
| Goat anti-FRIZZLED-6 polyclonal antibody | 1:200 | RyD Systems (Ref. AF1526) |
| Rabbit anti-CELSR1 polyclonal antibody | 1:200 | Millipore (Ref. 2398942) |
| Rabbit anti-VANGL1 polyclonal antibody | 1:200 | Sigma (Ref. HPA025235) |
| Rabbit anti-PRICKLE1 polyclonal antibody | 1:200 | Sigma (Ref. HPA001379) |
| Rabbit anti-PRICKLE3 polyclonal antibody | 1:200 | Sigma (Ref. HPA001442) |
| Rabbit anti-FAT1 polyclonal antibody | 1:200 | Sigma (Ref. HPA023882) |
| Mouse anti-Parvalbumin monoclonal antibody | 1:200 | Chemicon International (Ref. MAB1572) |
| Mouse anti-Prox1 monoclonal antibody | 1:200 | Sigma (Ref. P0089) |
| Mouse anti-SV2 monoclonal antibody | 1:200 | DSHB (Ref. AB_2315387) |
| Mouse anti-Glutamine Synthetase monoclonal antibody | 1:200 | Millipore (Ref. MAB302) |
| Mouse anti-ISLET1 (40.2D6) monoclonal antibody | 1:200 | DSHB (Ref. AB_528,315) |
| Mouse anti-β Tubulin III (neuronal) monoclonal antibody | 1:200 | Sigma (Ref. T8578-100UL) |
| Mouse anti-acetylated α Tubulin monoclonal antibody | 1:200 | Santa Cruz Biotechnology, INC. (Ref. Sc-23950) |
| **Secondary antibody** | **Working dilution** | **Antibodies suppliers** |
| Alexa Fluor 594 goat anti-rabbit IgG | 1:200 | Molecular Probes (Ref. A11037) |
| Alexa Fluor 488 anti-mouse IgG | 1:200 | Molecular Probes (Ref. A11029) |

### 2.4. Sequence analysis of PCP proteins

Protein ortholog sequences of FZD6, CELSR1, VANGL1, PK1, PK3, and FAT1 were retrieved using ENSEMBL web server from *Homo sapiens, Mus musculus, Gallus gallus, Danio rerio, and Drosophila melanogaster*. A multiple sequence alignment for each set of orthologs was generated using CLUSTAL and distances between each pair of sequences was estimated using the Neighbour-Joining algorithm.

## 3. Results

### 3.1. Immunohistochemical distribution PCP proteins in the laminated retina of Gallus gallus

We first analyzed the sequence conservation of the PCP proteins in *G. gallus* compared to other model species. Specifically, we assessed the molecular taxonomy of FZD6, CELSR1, VANGL1, PK1, PK3, and FAT1 in *Homo sapiens, Mus musculus, Danio rerio, and Drosophila melanogaster*. We observed a similar pattern among these proteins (Fig. S1), being *G. gallus* sequences more similar to human and murine proteins in comparison to fish or fly proteins. This result supports the idea of *G. gallus* as a model to study PCP proteins.

The distribution of PCP proteins in the developing *G. gallus* retina was carefully examined from E3, coinciding with the differentiation of the first ganglion cell neuroblasts (McCabe et al., 1999; Francisco--Morcillo et al., 2005; Bejarano-Escobar et al., 2015; de Mera-Rodríguez et al., 2019), to E15, an stage in which retinal cell types concluded their morphological differentiation and the different retinal layers were well established (Drenhaus et al., 2007; de Mera-Rodríguez et al., 2019). The chronotopographical distribution of PCP proteins in the developing retinal tissue followed a central-to-peripheral and a vitreal-to-scleral gradients, in concordance with the gradients described for retinogenesis in birds (Prada et al., 1991; Drenhaus et al., 2007; Álvarez-Hernán et al., 2018, 2021; de Mera-Rodríguez et al., 2019).

The patterns of staining for the different PCP proteins were first determined at E15 so as to establish a set of referents with which to compare the embryonic stages. Two of the proteins of the Fzd complex, Fzd6 (Fig. 1A–D) and Celsr1 (Fig. 1E-P), were immunolocalized in subpopulations of cells located in the GCL, amacrine cell layer, and horizontal cell layer. Some of the Fzd6-/Celsr1-immunoreactive cells located in the inner region of the INL were co-labeled with parvalbumin (PV) (Fig. 1A-L), a calcium binding protein that has been shown to be expressed in a subpopulation of amacrine cells in the developing and mature chicken retina (Sanna et al., 1992). These proteins were mainly located in the dendritic arbor extended towards the IPL (Fig. 1B'-D′, J-L). Furthermore, to explore the cellular localization of Fzd6 and Celsr1 in the outer region of the INL, we also used antibodies against Prox1, which label all horizontal cells in the avian retina (Edqvist et al., 2008; Boije et al., 2009; Álvarez-Hernán et al., 2021). Fzd6 (not shown) and Celsr1 (Fig. 1M–P) were found to co-label with Prox1 in the outer region of the INL (Fig. 1M–P).

Looking at the distribution of PCP proteins of the Vangl complex in the layered retina, a strong Vangl1 immunoreactivity was detected in cell processes located both in the IPL and in the OPL (Fig. 2A–H), that could be also identified with antibodies against SV2 (Fig. 2A–D), a marker of synaptic vesicles in the vertebrate retina (Bejarano-Escobar et al., 2014; Álvarez-Hernán et al., 2013, 2019, 2019; Pavón-Muñoz et al., 2016). Vangl1 immunoreactivity was also detected both in cells located in the GCL (Fig. 2A–H), in the layer where the cell somata of glutamine synthetase (GS)-immunoreactive Müller cells are located (Fig. 2E–H). Moreover, Vangl1 immunoreactivity was strongly detected in the photoreceptor layer (Fig. 2A–H).

Pk1 and Pk3 proteins showed similar distributions in the chicken laminated retina (Fig. 2I-P) and were detected in the GCL, amacrine cell layer, horizontal cell layer, and photoreceptor cell layer. Double labeling experiments showed that many PV-immunoreactive amacrine cells also

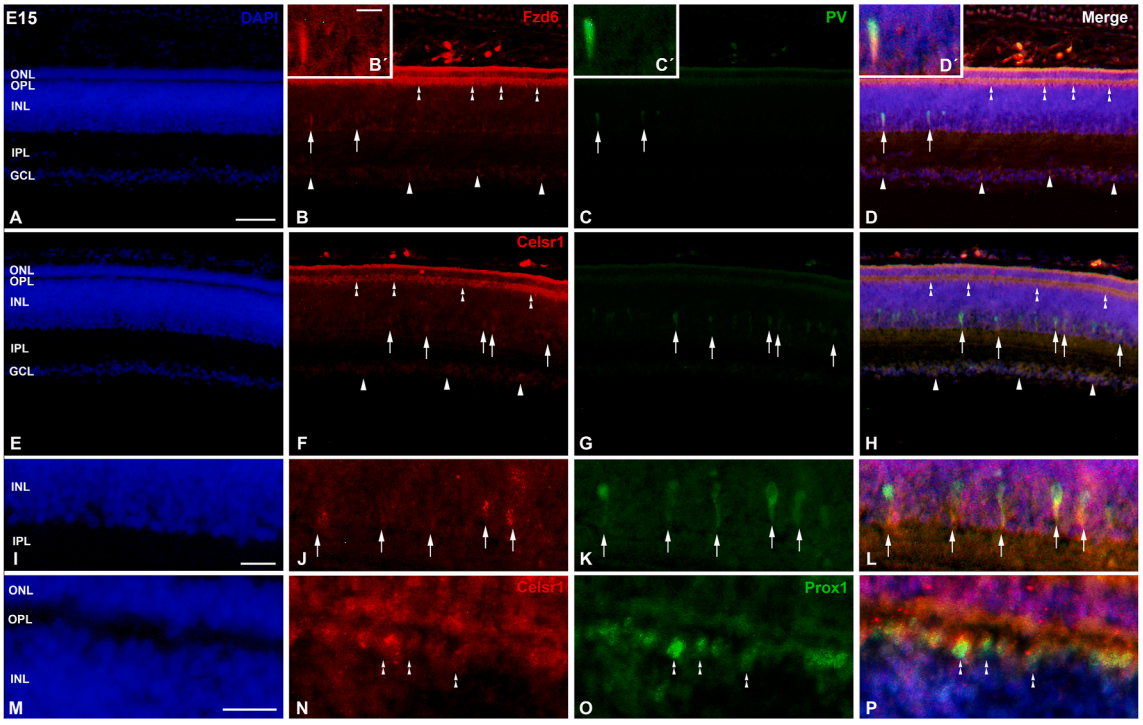


**Fig. 1.** Immunochemical analysis of Fzd6 (A–D) and Celsr1 (E–P) in the central region of the E15 chicken retina. DAPI staining (A,E,I,M) showed the multilayered structure of the retina. Both proteins were detected in the GCL (arrowheads), in a subpopulation of amacrine cells (arrows), and in the horizontal cell layer (double arrowheads). Double labeling Fzd6/PV (A–D), Celsr1/PV (E–L) and Celsr1/Prox1 (M–P) revealed a partial co-expression of these proteins in a subpopulation of amacrine (arrows in B-D, F–H, J-L) and horizontal cells (double arrowheads in N–P) respectively. *GCL, ganglion cell layer; INL, inner nuclear layer; IPL, inner plexiform layer; ONL, outer nuclear layer; OPL, outer plexiform layer.* Scale bars: 50 μm in A-H; 5 μm in B'-D'; 25 μm in I-L, and M-P.

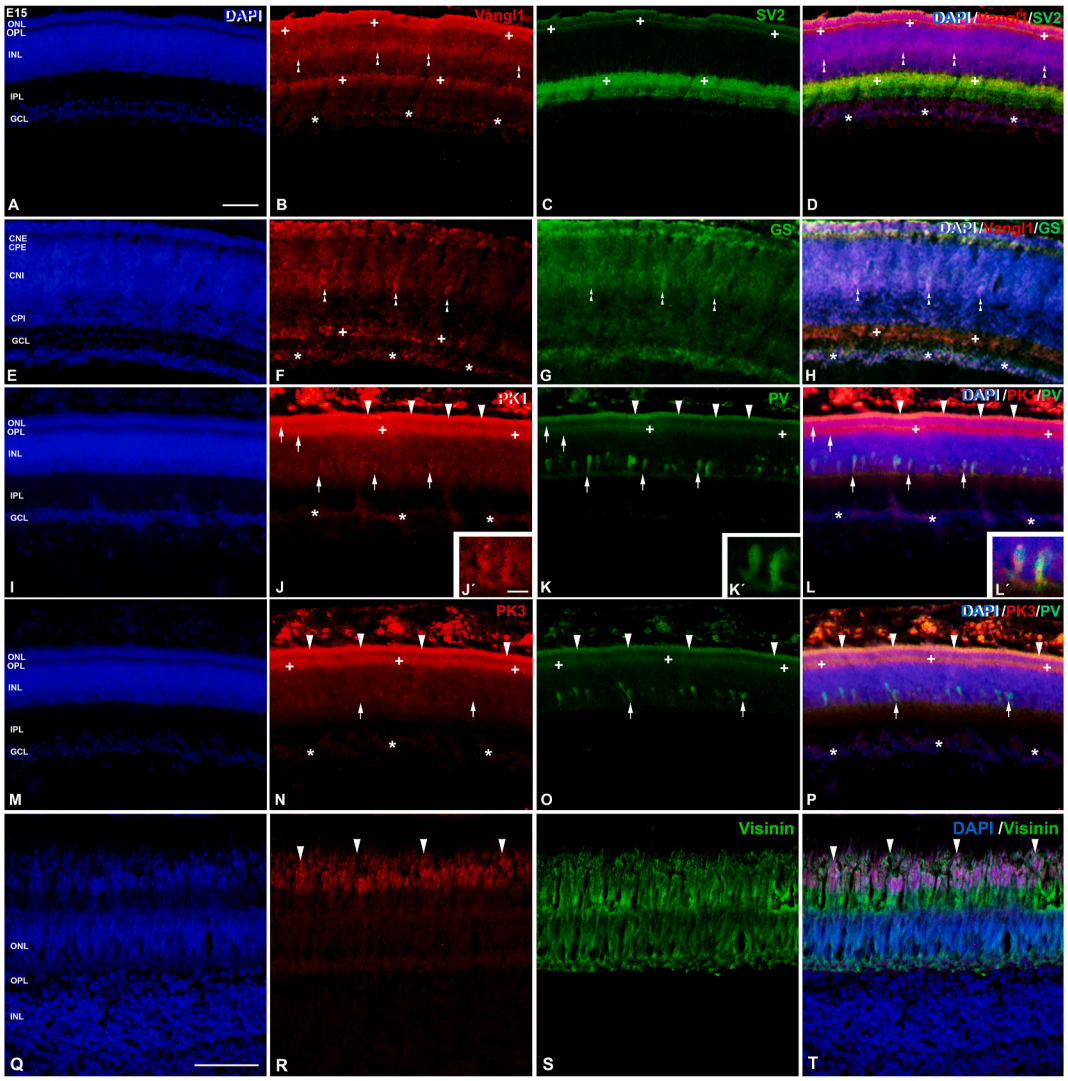


**Fig. 2.** Distribution of Vangl1 (A–H), Pk1 (I–L) and Pk3 (M–T) in the central region of the E15 chicken retina. DAPI staining (A,E,I,M,Q) showed the multilayered structure of the retina. These PCP proteins were all detected in the GCL (asterisks) and in the photoreceptor cell layer (arrowheads). Strong Vangl1 immunoreactivity co-express with SV2 labeling in the IPL and OPL (crosses in B-D). Vangl1 was detected in the cell bodies of GS-immunoreactive Müller cells (double arrowheads in F–H). Pk1 and Pk3 proteins were found in a subset of PV-immunoreactive amacrine cells (arrows in I–P) and in the horizontal cell layer (triple arrowheads). Pk3 immunoreactivity in the ONL was restricted to the outer segments of visinin-positive photoreceptors (arrowheads in Q-T). *GCL, ganglion cell layer; INL, inner nuclear layer; IPL, inner plexiform layer; ONL, outer nuclear layer; OPL, outer plexiform layer.* Scale bars: 50 μm in A-P; 5 μm in J'-L'; 25 μm in Q-T.

expressed PK1 (Fig. 2I-L) and PK3 (Fig. 2M–P). To identify the photoreceptors in the developing and mature retina of birds, the antibody against visinin has been widely used (Bruhn and Cepko, 1996; Álvarez-Hernán et al., 2020; 2021). We found visinin+/Pk1+ (not shown) and visinin+/Pk3+ photoreceptors (Fig. 2Q–T) in the laminated chicken retina. However, while visinin was expressed in the entire photoreceptor cell body (Fig. 2S,T), Pk1 and Pk3 proteins were restricted to the outer segments of these cells (Fig. 2R,T).

Regarding the Ft-Ds pathway, the expression of the protocadherin Fat1 was detected in the GCL (Fig. 3B–D; F–H). Furthermore, double immunohistochemistry revealed that some of the Fat1-immunoreactive amacrine cells also expressed PV (Fig. 3B–D). In the more external retina, Fat1 immunoreactivity was detected in the OPL, externally to the Prox1-immunoreactive horizontal cell somata (Fig. 3E–H; F'-H′).

### 3.2. *Distribution of the PCP components in the developing retina of Gallus gallus*

In the undifferentiated retina of E3 embryos, Fzd6-, Celsr1-, and Vangl1-proteins were mainly located in the vitreal and in the scleral surface of the neuroblastic layer (NbL) (Fig. 4). At E6, the neural retina was still composed of a NbL and the Fzd6-/Celsr1-labeling became more intense in cell somata located in the vitreal surface (Fig. 5A–G). Most of the Celsr1 immunoreactive cells located in the most-vitreal region of the NbL were also labeled with the transcription factor Isl1 (Fig. 5D–G, E'-G′), that is expressed by differentiating ganglion cells (Álvarez-Hernán et al., 2013; Martin-Partido and Francisco-Morcillo, 2015; Bejarano-Escobar et al., 2015; Luo et al., 2019). Isl1-immunoreactive migrating neuroblasts located in more external layers did not express Celsr1 (Fig. 5E–G). Faint immunoreactivity against Fzd6 and Celsr1 was found in the optic fibre layer (OFL), that appeared strongly labeled with antibodies against α-Tubulin-(α-Tub) (Fig. 5H–K), a ganglion cell axon marker in the developing and mature vertebrate retina (Sale et al., 1988; Senut et al., 2004; Fausett and Goldman, 2006).

On the contrary, at E6 Vangl1 immunoreactivity was mainly restricted to the OFL and to the presumptive photoreceptor cell layer (Fig. 6). We also detected in Vangl1-positive axons other early markers of ganglion cell axons in the developing avian retina (Snow and Robson,

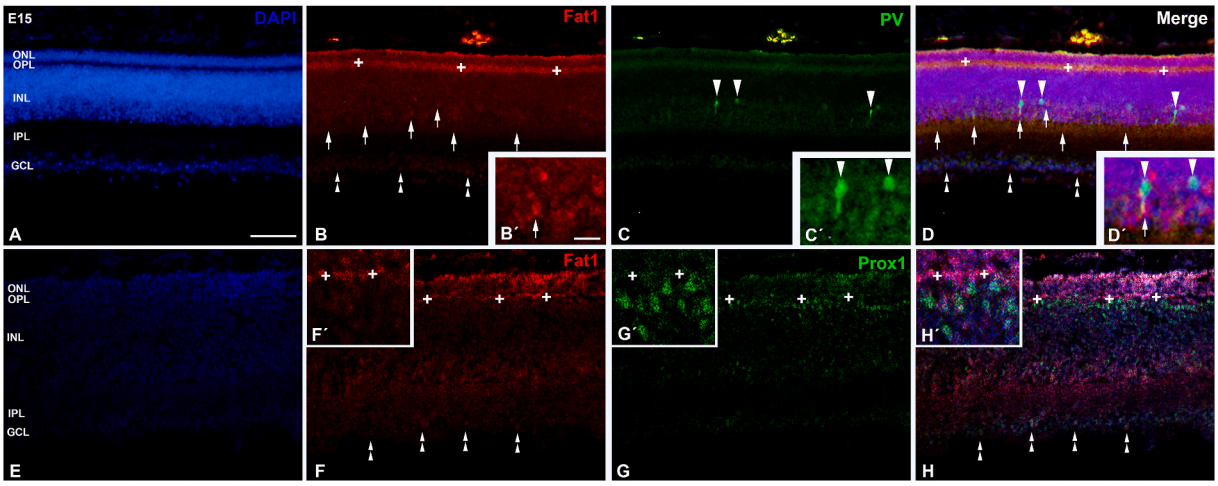


**Fig. 3.** Distribution of Fat1 in the central region of the E15 chicken retina. DAPI staining (A,E) showed the multilayered structure of the retina. Fat1 immunoreactivity was found in the GCL (double arrowheads), in a subset of amacrine cells (arrows), some of them also immunoreactive against PV (arrowheads) and in the OPL (crosses), externally to the Prox1-immunoreactive horizontal cell somata (E–H). *GCL, ganglion cell layer; INL, inner nuclear layer; IPL, inner plexiform layer; ONL, outer nuclear layer; OPL, outer plexiform layer.* Scale bars: 50 μm in A-H; 5 μm in B'-D'.

1994; Bergmann et al., 1999; Álvarez-Hernán et al., 2021), such as tubulin β class III (TUJ1) (Fig. 6D–G) and SV2 (Fig. 6H-O). Double immunolabeling techniques also demonstrated that Vangl1-immunoreaction was detected earlier in growing axons than SV2 (Fig. 6L–O). Pk1 and Pk3 proteins presented similar distribution in the undifferentiated chicken retina (Fig. 7). At E3, these proteins were mainly restricted to the vitreal surface (Fig. 7A–C; G-I), while in the E6 retina stained cell bodies located in the vitreal and scleral surfaces (Fig. 7D–F; J-L).

At E8, Fzd6, Celsr1, Vangl1, Pk1 (Fig. S2), and Pk3 (not shown) showed a similar staining patterns to those described in the E15 retina. However, Vangl1 immunoreactivity was still absent in the Müller cell somata (Figs. S2G–J). Müller cells in the developing chicken retina constitute the cell type that differentiated last (Prada et al., 1991), and the earlier specific cell markers were found at E11 (Linser and Moscona, 1981; Doh et al., 2010).

The protocadherin Fat1 was immunodetected in the vitreal surface of the E3 chicken retina (Fig. 8A–C). At E6, Fat1 immunoreactivity was mainly detected in cell somata located near the vitreal surface of the NbL (Fig. 8D–F). As development proceeded, the overall number of Fat1-immunoreactive cells increased and by E8 (Fig. 8G–I) included cells located in the GCL and in the inner region of the INL. Strong immunoreactivity against Fat1 was also detected in the OPL (Fig. 8G–I).

Therefore, most of the PCP proteins described in the present study were detected very early during development of the chicken retina. Many of them were strongly expressed in the ganglion and amacrine cells. Some of them were also found in the dendrites and axons located in the plexiform layers and in the OFL. All these data are summarized in Fig. 9 and Table S3.

## 4. Discussion

Here we provide a detailed description of the spatiotemporal expression of different PCP components in the developing avian retina. To our knowledge, this is the first report in which is described the protein distribution of Celsr1, Vangl1, Pk3, and Fat1 in the retina of vertebrates, and the immunohistochemical pattern of Fzd6 and Pk1 in the avian retina. We observed that these proteins are expressed in a tissue and cell-specific fashion. Most of them are detected very early in axons emerging from differentiating ganglion cells and in their cell somata. Subpopulations of amacrine and horizontal cells also expressed many of the PCP proteins included in the present study. Finally, some of them are located in Müller cells, in specific segments of the photoreceptor cells and in the plexiform layers.

All these results are discussed below, comparing their expression patterns in the developing chicken retina with those previously described in other vertebrate retinas for the same proteins or proteins from their families. Finally, attending to their chronotopographical expression during development, we suggest some possible roles for these proteins in retinogenesis and maintenance of retinal phenotypes.

### 4.1. *Fzd6*

Intense Fzd6 immunoreactivity was found in the ganglion cell somata and their axons in the early developing and mature chicken retina, in concordance with results obtained in mice (Liu et al., 2003; de Iongh et al., 2006). However, immunoreactivity against this protein in amacrine and horizontal cells has never been described in the vertebrate retina. The staining pattern observed in the chicken retina for Fzd6 is very similar to that described for Fzd3, other member of the Fzd family, shows an identical distribution in the developing and mature mouse retina (Shen et al., 2016). Other family members such as Fzd5 and Fzd8 were also found in a subset of amacrine cells in the developing mouse (Liu and Nathans, 2008; Liu et al., 2012).

It has been demonstrated that ganglion cells differentiate normally and amacrine and horizontal cells stratify correctly in the plexiform layer in *Fzd3* KO mouse (Hua et al., 2014; Shen et al., 2016). Similarly, retinal neurons in KO mice for *Fzd8* were developed correctly (Liu and Nathans, 2008). Therefore, Fzd3 and Fzd8 seem not to be required for differentiation and maintenance of phenotypes of these retinal cell types. Fzd6 and Fzd3 show a similar distribution in the vertebrate retina, but also in other neural systems. They share redundant functions regulating neural tube closure and the planar orientation of hair bundles in the auditory and vestibular sensory cells (Wang et al., 2006). Furthermore, they also control the establishment of axonal projections in the CNS (Hua et al., 2013). All these results suggest that Fzd6 and Fzd3 could act redundantly in control different developmental processes during retinal development.

### 4.2. *Celsr1*

*Celsr* cadherins (*Celsr1, Celsr2, and Celsr3)* are ubiquitously expressed in many tissues during development (Wang et al., 2014), including the CNS (Tissir and Goffinet, 2006). In the case of the developing retina, it has been described Celsr3 expression pattern and function in the zebrafish (Lewis et al., 2011, 2015), but the distribution of other family

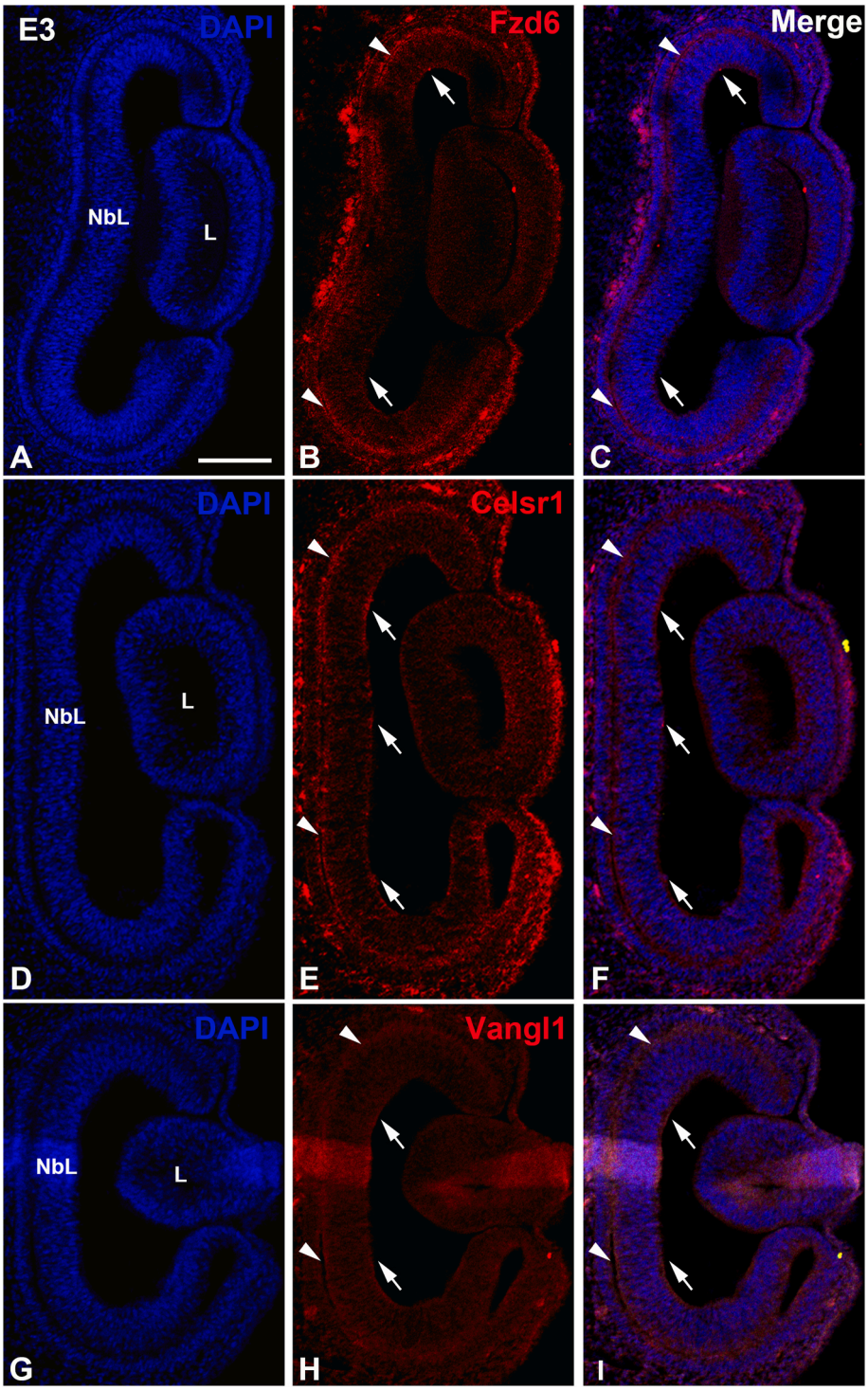


**Fig. 4.** Distribution of Fzd6 (A–C), Celsr1 (D–F), and Vangl1 (G–I) in the E3 chicken retina. DAPI staining (A,D,G) showed that neural retina was composed of a NbL. PCP-components were restricted to the vitreal (arrows) and scleral (arrowheads) surfaces of the undifferentiated retina. *L, lens; NbL, neuroblastic layer.* Scale bar: 100 μm.

members in this tissue, such as Celsr1, remained unknown. Celsr1 immunohistochemistry in the E3-E6 chicken retina revealed staining in the presumptive GCL and in the NFL. As development proceeded, Celsr1 was also localized in amacrine and horizontal cells. In the zebrafish retina, *Celsr3* shows a similar staining pattern, being detected in the GCL and in the amacrine cell layer, but in contrast, is absent from horizontal cells (Lewis et al., 2011, 2015).

Celsr1 and Celsr3 are closely related to some processes in neural development, such as dendritic and axon development or neuronal migration (Qu et al., 2010; Feng et al., 2012). Therefore, these proteins could be functionally implicated in proper dendritic and axonal targeting in these neuronal cell types in the vertebrate retina.

### 4.3. *Vangl1*

Vangl1 immunoreactivity has not previously been described in the

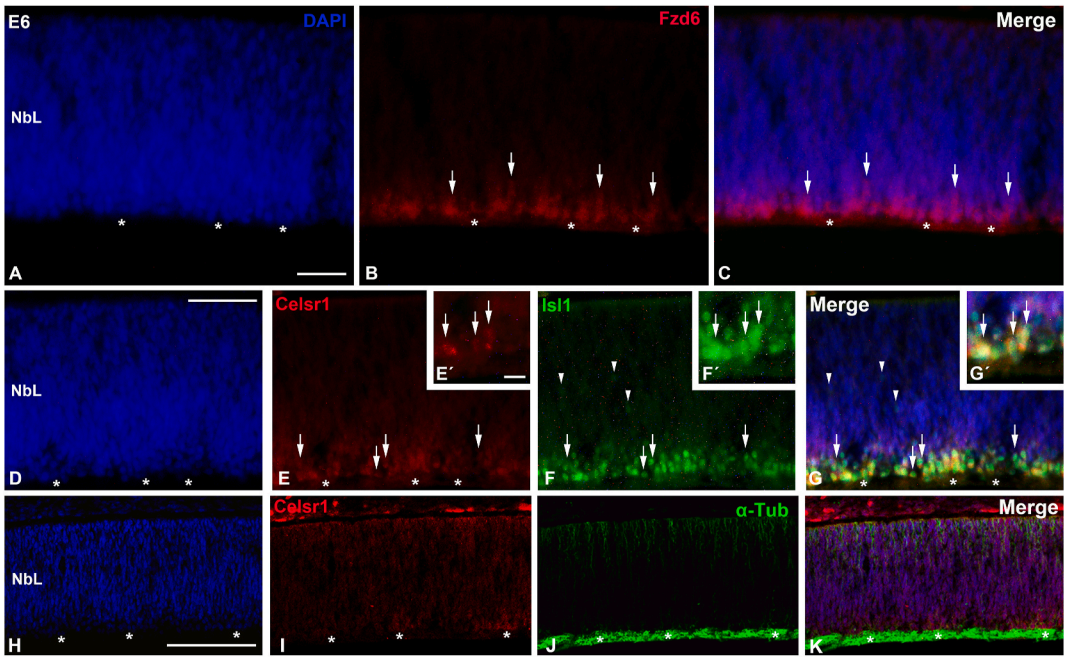


**Fig. 5.** Distribution of Fzd6 (A–C) and Celsr1 (D–K) in the E6 chicken retina. DAPI staining (A,D,H) showed that neural retina was composed of a NbL. Fzd6-immunoreactivity was restricted to cell somata located in the vitreal region of the NbL (arrows) and to the OFL (asterisks). Cels1 immunoreactivity revealed a partial co-expression with Isl1 immunoreactive nuclei (arrows in G). Isl1-immunoreactive migrating neuroblasts (arrowheads) were also negative for Celsr1 labeling. α-Tub immunoreactive ganglion cell axons located in the OFL appeared faintly labeled with antibodies against Celsr1 (asterisks in I). *NbL, neuroblastic layer.* Scale bars: 25 μm in A-C; D-G; 5 μm in E'-G'; 50 μm in H–K.

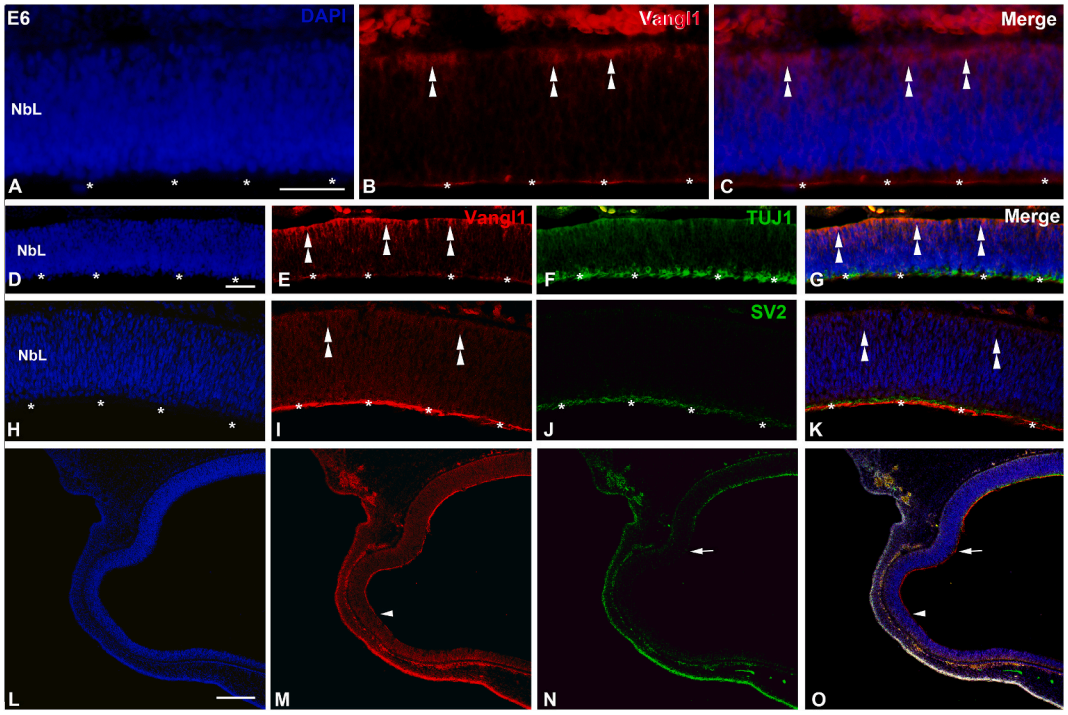


**Fig. 6.** Distribution of Vangl1 in the E6 chicken retina. DAPI staining (A,D,H,L) showed that neural retina was composed of a NbL. Vangl1-immunoreactivity was detected in the OFL (asterisks) and in the presumptive photoreceptor cell layer (double arrowheads). Vangl1 immunoreactive ganglion cell axons were also labeled with antibodies against TUJ1 (asterisks in E-G). Optic axons were also immunoreactive against SV2 (H–O), but Vangl1-immunoreactivity (arrowheads in M,O) was detected in more peripheral regions than SV2 labeling (arrows in N,O). *NbL, neuroblastic layer.* Scale bars: 25 μm in A-C; D-K. 100 μm in L-O.

vertebrate retinal tissue. This protein was detected in the NbL and in the three nuclear layers of the laminated retina. During early stages of retinogenesis, it was detected in early ganglion cell axons, showing a similar location to that described for Vangl2 in the NbL of the mouse retina (Torban et al., 2007; Leung et al., 2015). Those authors demonstrated that Vangl2 could be considered as an early marker of ganglion cell axons. In the present study, we demonstrated that Vangl1 was detected in axons emerging from newborn ganglion cells earlier than

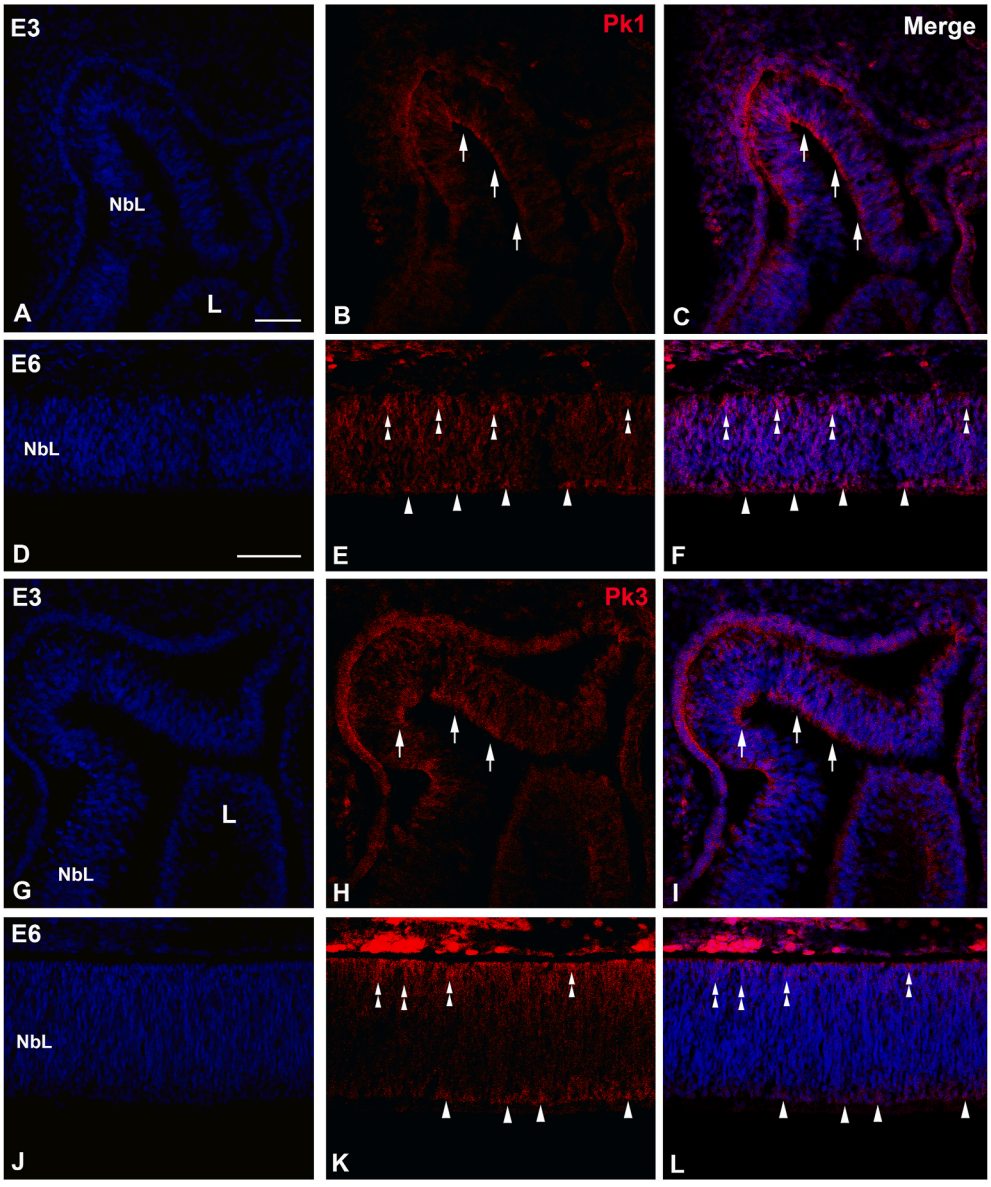


**Fig. 7.** Distribution of Pk1 (A–F) and Pk3 (G–L) in the E3 (A-C; G-I) and E6 (D-F; J-L) chicken retina. DAPI staining (A,D,G,J) showed that neural retina was composed of a NbL. At E3, Pk1 was restricted to the vitreal surface of the NbL (arrows). At E6, Pk1 immunoreactivity concentrates in cell somata located both in the vitreal (arrowheads in E-F) and scleral (double arrowheads in E-F) of the NbL. Pk3 showed identical pattern of immunoreactivity by these early stages (arrows, arrowheads, and double arrowheads in G-L). *L, Lens; NbL, neuroblastic layer*. Scale bars: 100 μm in A-C; G-I; 50 μm in D-F, J-L.

SV2, an early marker of ganglion cell differentiation in the developing retina of fish (Bejarano-Escobar et al., 2010, 2012, 2012; Pavón-Muñoz et al., 2016), amphibians (Álvarez-Hernán et al., 2013), birds (Bergmann et al., 1999; Álvarez-Hernán et al., 2018), and mammals (Okada et al., 1994). Therefore, both proteins were detected in emerging ganglion cell axons in the vertebrate retina.

In the laminated retina, Vangl1 was also detected in the ganglion cell somata in the developing chicken retina. *Vangl1* mRNA was present in most of the cells located in the GCL in the larval retina of zebrafish (Jessen and Solnica-Krezel, 2004), but was absent in the cell somata of ganglion cells in the mouse retina (Tissir and Goffinet, 2006). Vangl1 signal was also detected in the middle part of the INL co-localizing with GS. It was only detected in E15 chicken retinas because Müller cells are the last cell type generated during retinogenesis in birds (Prada et al., 1991). Most of the PCP components are restricted to retinal neural lineage, with the exception of Fzd5 (Liu and Nathans, 2008), Fat1 (Helmbacher, 2020), and Vangl1 (present study) that are expressed in Müller glia and astrocytes in the retinal tissue. Finally, Vangl1 was strongly expressed in the developing and mature chicken photoreceptor layer. Immunohistochemistry using Vangl1 antibodies clearly showed that this protein was restricted to outer segments of the mature chicken photoreceptors. Again, Vangl2 mRNA expression is strongly detected in the photoreceptor layer in the larval zebrafish retina (Song et al., 2016). These authors demonstrated that Vangl2 and Arl13 b interact in a specific protein complex essential for photoreceptor outer segment development and stability.

All these data clearly show that Vangl1 (present study) and Vangl2 (Leung et al., 2015; Song et al., 2016) show a similar staining pattern in the developing and mature vertebrate retina, with the exception of the Vangl1 expression in the Müller cells. It has also been described that Vangl1 and Vangl2 are coexpressed in many areas of the embryo, such as the cochlea, heart, skin, and kidneys (Torban et al., 2008). Many authors also suggest redundant functions for both proteins during development of the CNS (Torban et al., 2008; Belotti et al., 2012; Song et al., 2016). Belotti et al. (2012) demonstrated that both proteins could interact physically to form an active protein complex. Therefore, in the developing retina, these results may suggest that both proteins could interact to regulate key roles attributed to Vangl2, such as early axon guidance or projections of retinal neurons throughout the INL and the ONL (Leung et al., 2015). However, additional experimentation will be required to test this hypothesis at the molecular level.

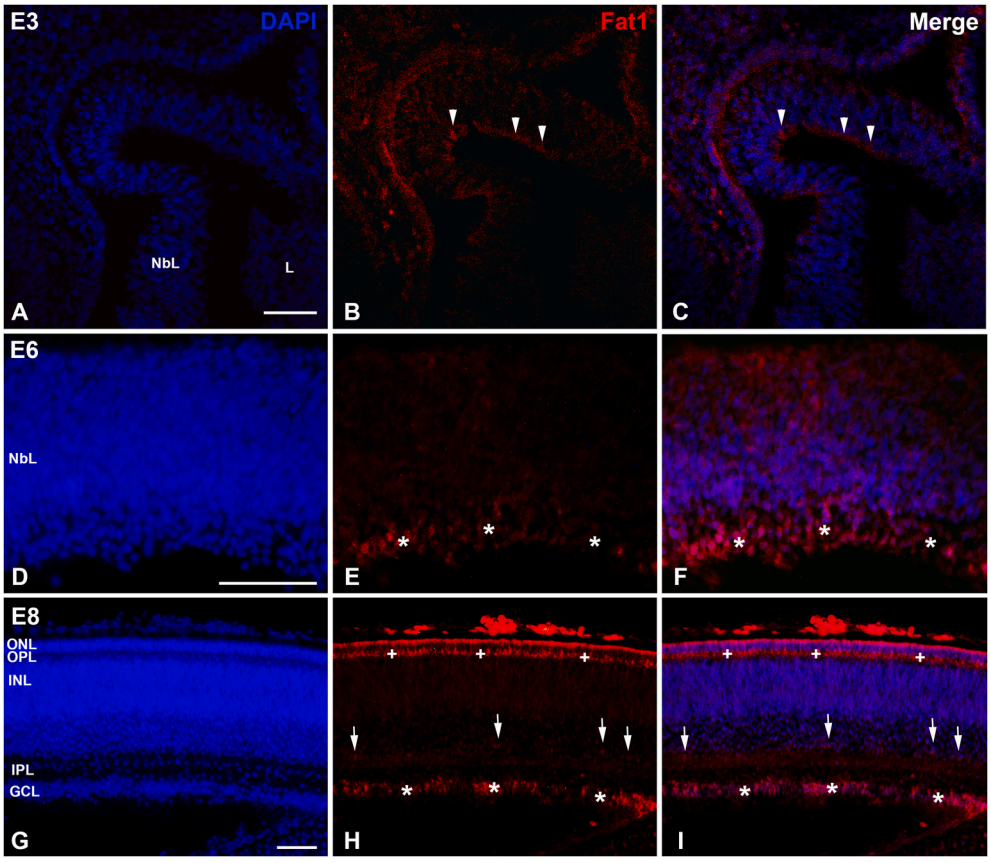


**Fig. 8.** Distribution of Fat1 in the E3 (A–C), E6 (D–F), and E8 (G–I). DAPI staining (A,D, G) showed the cytoarchitecture of the neural retina. At E3 (A–C) Fat1 was expressed in the vitreal surface of the retina (arrowheads). Fat1 immunoreactive ganglion cells were detected at E6 (asterisks in D-F) and E8 (asterisks in G-I). At E8, Fat1 immunoreactivity extended to a subset of amacrine cells (arrows) and to the OPL (crosses in G-I). *GCL, ganglion cell layer; INL, inner nuclear layer; IPL, inner plexiform layer; NbL, neuroblastic layer; ONL, outer nuclear layer; OPL, outer plexiform layer.* Scale bars: 100 μm in A-C; 50 μm in D-F and G-I.

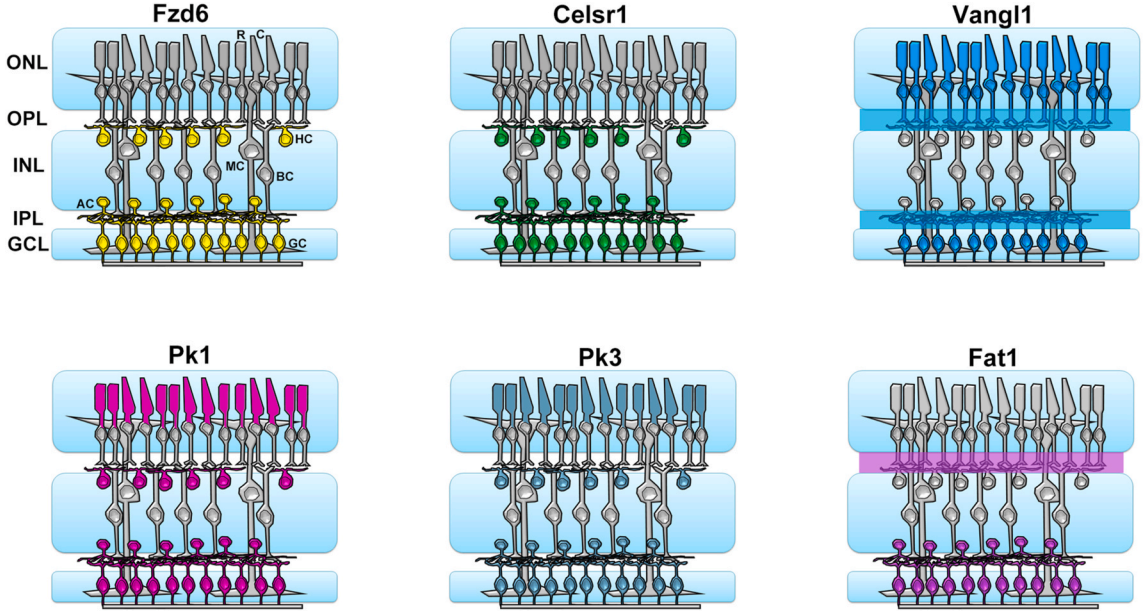


**Fig. 9.** Distribution of Fzd6 (A), Celsr1 (B), Vangl1 (C), Pk1 (D), Pk3 (E), and Fat1 (F) in the laminated chicken retina. Labeled retinal elements appear coloured in the scheme. *AC, amacrine cell; BC, bipolar cell; GCL, ganglion cell layer; GC, ganglion cell; HC, horizontal cell; INL, inner nuclear layer; IPL, inner plexiform layer; MC, Müller cell; ONL, outer nuclear layer; OPL, outer plexiform layer.*

### *4.4. Pk1 and Pk3*

For the Pk family, Pk1 and Pk3 showed identical immunoreactivity in the developing chicken retina. The results obtained for Pk1 in the chicken retina were highly coincident with those described for the same protein in the developing and mature mouse retina (Liu et al., 2013). Pk1 is detected in both species in early differentiating ganglion cells and their axons. At more advanced stages, Pk1 expression in the INL is restricted to a subpopulation of amacrine cells, in a subpopulation of amacrine neurons the newborn was also detected in a subpopulation of

amacrine neurons that has been identified as cholinergic starburst amacrine cells in the mouse (Liu et al., 2013). Finally, Pk1 was detected in differentiating chicken photoreceptors and restricted to the outer segments of these cells in E15 retinas. In the mouse, Pk1 is weakly expressed throughout the ONL (Liu et al., 2013). These authors also found that *Pk1* knock-down in the neonatal retina leads to defects in inner and outer segments of photoreceptors, suggesting a role for this PCP component in rod photoreceptor morphogenesis.

Concerning the results obtained to Pk3, its staining pattern has never been described in the vertebrate retina. Recently, it has been shown that Pk3 KO mouse displayed retinal deficiencies, such as significant decreases in the number of RGCs and abnormal vasculature (Yu et al., 2020), and therefore, this protein could be involved in ocular morphogenesis during development.

### 4.5. *Fat1*

Although several studies described the distribution and the possible implication of Fat3 in retinal development, little is known about Fat1 in this tissue and, to our knowledge, this is the first study in which is described the chronotopographical distribution of this protein in the developing visual system of vertebrates. Fat1 was immunodetected in the early differentiating ganglion cell somata and their axons, coinciding with the *Fat3* mRNA and protein distributions in the mouse GCL at perinatal and postnatal stages (Nagae et al., 2007; Deans et al., 2011). Fat1 was also localized to the portion of the leading process of amacrine cells in the chicken retina. Fat3 is also asymmetrically localized in the dendritic processes of amacrine cells that expands into the IPL (Nagae et al., 2007; Krol et al., 2016; Horne-Badovinac, 2017) and is a critical regulator of dendrite morphogenesis in amacrine cells and their migration in the mouse retina (Deans et al., 2011). Therefore, Fat1 and Fat3 distributions are highly coincident in the vertebrate retina, except for the strong expression detected in the OPL for Fat1, that was absent in the laminated mouse retina (Nagae et al., 2007).

## 5. Conclusions

Taken together, our results clearly show that PCP proteins are specifically distributed in the retina at different stages of development and show a complex and partially overlapping immunohistochemical patterns. Their distribution at early stages of retinogenesis suggest that they may provide a combinatorial adhesive code that favors the guidance of retinal ganglion cells throughout the visual pathways. This PCP signaling influence on axon guidance has previously been described in the developing CNS (Davey and Moens, 2017; Onishi et al., 2020). Furthermore, the asymmetrical distribution of some of these proteins in differentiating retinal cell types may suggest an additional possible role in the genetic regulation of neuronal morphogenesis in amacrine and photoreceptor cells (Deans et al., 2011; Liu et al., 2013).

## Ethics approval

All animals were treated according to the regulations of the European Union 130 (EU Directive, 2010/63/EU) and Spain (Royal Decree 53/2013).

## Funding

This work was supported by grants from the Spanish *Ministerio de Ciencia y Tecnología* (BFU 2007-67540), *Dirección General de Investigación del Ministerio de Educación y Ciencia* (BFU 2017-85547-P), and Junta de Extremadura, *Fondo Europeo de Desarrollo Regional, "Una manera de hacer Europa"* (GR15158, GR18114, IB18113).

## Authors' contributions

JMCG and JFM designed research, ACR, SGJ and GAH analyzed data; GAH and SGJ performed research; LC, AP, JMCG and JFM wrote the paper.

## Availability of data and material

The data and material can be freely given upon request.

## Code availability

The code can be freely given upon request.

## Declaration of competing interest

The authors declare that they have no conflict of interest.

## Acknowledgements

The authors acknowledge the support of the *Servicio de Técnicas Aplicadas a las Biociencias* (STAB-SAIUEX) of the Universidad de Extremadura.

## Appendix A. Supplementary data

Supplementary data related to this article can be found at https://doi.org/10.1016/j.exer.2021.108681.

## References

Álvarez-Hernán, G., Andrade, J.P., Escarabajal-Blázquez, L., Blasco, M., Solana-Fajardo, J., Martín-Partido, G., Francisco-Morcillo, J., 2019. Retinal differentiation in syngnathids: comparison in the developmental rate and acquisition of retinal structures in altricial and precocial fish species. Zoomorphology 138, 371–385.

Álvarez-Hernán, G., Bejarano-Escobar, R., Morona, R., González, A., Martin-Partido, G., Francisco-Morcillo, J., 2013. Islet-1 immunoreactivity in the developing retina of Xenopus laevis. The ScientificWorld Journal 2013 11.

Álvarez-Hernán, G., de Mera-Rodríguez, J.A., Gañán, Y., Solana-Fajardo, J., Martín-Partido, G., Rodríguez-León, J., Francisco-Morcillo, J., 2021. Development and postnatal neurogenesis in the retina: a comparison between altricial and precocial bird species. Neural Regeneration Research 16, 16.

Álvarez-Hernán, G., Hernández-Núñez, I., Rico-Leo, E.M., Marzal, A., de Mera-Rodríguez, J.A., Rodríguez-León, J., Martín-Partido, G., Francisco-Morcillo, J., 2020. Retinal differentiation in an altricial bird species, Taeniopygia guttata: an immunohistochemical study. Exp. Eye Res. 190, 14.

Álvarez-Hernán, G., Sánchez-Resino, E., Hernández-Núñez, I., Marzal, A., Rodríguez-León, J., Martín-Partido, G., Francisco-Morcillo, J., 2018. Retinal histogenesis in an altricial avian species, the zebra finch (Taeniopygia guttata, Vieillot 1817). J. Anat. 233, 106–120.

Axelrod, J.D., 2020. Planar cell polarity signaling in the development of left–right asymmetry. Curr. Opin. Cell Biol. 62, 61–69.

Bastock, R., Strutt, H., Strutt, D., 2003. Strabismus is asymmetrically localised and binds to Prickle and Dishevelled during Drosophila planar polarity patterning. Development 130, 3007–3014.

Bejarano-Escobar, R., Álvarez-Hernán, G., Morona, R., González, A., Martin-Partido, G., Francisco-Morcillo, J., 2015. Expression and function of the LIM-homeodomain transcription factor Islet-1 in the developing and mature vertebrate retina. Exp. Eye Res. 138, 22–31.

Bejarano-Escobar, R., Blasco, M., Degrip, W.J., Oyola-Velasco, J.A., Martin-Partido, G., Francisco-Morcillo, J., 2010. Eye development and retinal differentiation in an altricial fish species, the senegalese sole (Solea senegalensis, Kaup 1858). J. Exp. Zool. B Mol. Dev. Evol. 314, 580–605.

Bejarano-Escobar, R., Blasco, M., Duran, A.C., Rodríguez, C., Martin-Partido, G., Francisco-Morcillo, J., 2012. Retinal histogenesis and cell differentiation in an elasmobranch species, the small-spotted catshark Scyliorhinus canicula. J. Anat. 220, 318–335.

Bejarano-Escobar, R., Blasco, M., Martin-Partido, G., Francisco-Morcillo, J., 2014. Molecular characterization of cell types in the developing, mature, and regenerating fish retina. Rev. Fish Biol. Fish. 24, 31.

Belotti, E., Puvirajesinghe, T.M., Audebert, S., Baudelet, E., Camoin, L., Pierres, M., Lasvaux, L., Ferracci, G., Montcouquiol, M., Borg, J.P., 2012. Molecular characterisation of endogenous Vangl2/Vangl1 heteromeric protein complexes. PloS One 7 e46213.

Bergmann, M., Grabs, D., Rager, G., 1999. Developmental expression of dynamin in the chick retinotectal system. J. Histochem. Cytochem. 47, 1297–1306.

Boije, H., Edqvist, P.H., Hallböök, F., 2009. Horizontal cell progenitors arrest in G2-phase and undergo terminal mitosis on the vitreal side of the chick retina. Dev. Biol. 330, 105–113.
Bruhn, S.L., Cepko, C.L., 1996. Development of the pattern of photoreceptors in the chick retina. J. Neurosci. 16, 1430–1439.
Butler, M.T., Wallingford, J.B., 2017. Planar cell polarity in development and disease. Nat. Rev. Mol. Cell Biol. 18, 375.
Butler, M.T., Wallingford, J.B., 2018. Spatial and temporal analysis of PCP protein dynamics during neural tube closure. eLife. 2018;7:e36456. doi:10.7554/eLife.36456.001.
Caruso, N., Herberth, B., Bartoli, M., Puppo, F., Dumonceaux, J., Zimmermann, A., Denadai, S., Lebossé, M., Roche, S., Geng, L., 2013. Deregulation of the protocadherin gene FAT1 alters muscle shapes: implications for the pathogenesis of facioscapulohumeral dystrophy. PLoS Genet. 9 e1003550.
Ciani, L., Patel, A., Allen, N.D., 2003. Mice lacking the giant protocadherin mFAT1 exhibit renal slit junction abnormalities and a partially penetrant cyclopia and anophthalmia phenotype. Mol. Cell Biol. 23, 3575–3582.
da Costa Calaza, K., Gardino, P.F., 2010. Neurochemical phenotype and birthdating of specific cell populations in the chick retina. An. Acad. Bras. Cienc. 82, 595–608.
Das, G., Reynolds-Kenneally, J., Mlodzik, M., 2002. The atypical cadherin Flamingo links Frizzled and Notch signaling in planar polarity establishment in the Drosophila eye. Dev. Cell 2, 655–666.
Davey, C.F., Moens, C.B., 2017. Planar cell polarity in moving cells: think globally, act locally. Development 144, 187–200.
de Iongh, R.U., Abud, H.E., Hime, G.R., 2006. WNT/Frizzled signaling in eye development and disease. Front. Biosci. : J. Vis. Literacy 11, 2442–2464.
de Mera-Rodríguez, J.A., Álvarez-Hernán, G., Gañán, Y., Martín-Partido, G., Rodríguez-León, J., Francisco-Morcillo, J., 2019. Senescence-associated β-galactosidase activity in the developing avian retina. Dev. Dynam. 248, 15.
Deans, M.R., Krol, A., Abraira, V.E., Copley, C.O., Tucker, A.F., Goodrich, L.V., 2011. Control of neuronal morphology by the atypical cadherin Fat3. Neuron 71, 820–832.
Devenport, D., 2014. The cell biology of planar cell polarity. JCB (J. Cell Biol.) 207, 171–179.
Doh, S.H., Kim, J.H., Lee, K.M., Park, H.Y., Park, C.K., 2010. Retinal ganglion cell death induced by endoplasmic reticulum stress in a chronic glaucoma model. Brain Res. 1308, 158–166.
Drenhaus, U., Morino, P., Rager, G., 2004. Expression of axonin-1 in developing amacrine cells in the chick retina. J. Comp. Neurol. 468, 496–508.
Drenhaus, U., Morino, P., Veh, R.W., 2003. On the development of the stratification of the inner plexiform layer in the chick retina. J. Comp. Neurol. 460, 1–12.
Drenhaus, U., Voigt, T., Rager, G., 2007. Onset of synaptogenesis in the plexiform layers of the chick retina: a transmission electron microscopic study. Microsc. Res. Tech. 70, 329–335.
Duncan, J.S., Stoller, M.L., Francl, A.F., Tissir, F., Devenport, D., Deans, M.R., 2017. Celsr1 coordinates the planar polarity of vestibular hair cells during inner ear development. Dev. Biol. 423, 126–137.
Edqvist, P.H., Lek, M., Boije, H., Lindback, S.M., Hallböök, F., 2008. Axon-bearing and axon-less horizontal cell subtypes are generated consecutively during chick retinal development from progenitors that are sensitive to follistatin. BMC Dev. Biol. 8, 46.
Fausett, B.V., Goldman, D., 2006. A role for alpha 1 tubulin-expressing Muller glia in regeneration of the injured zebrafish retina. J. Neurosci. : the official journal of the Society for Neuroscience 26, 6303–6313.
Feng, J., Han, Q., Zhou, L., 2012. Planar cell polarity genes, Celsr1-3, in neural development. Neuroscience bulletin 28, 309–315.
Francisco-Morcillo, J., Sánchez-Calderon, H., Kawakami, Y., Belmonte, J.C., Hidalgo-Sánchez, M., Martín-Partido, G., 2005. Expression of Fgf 19 in the developing chick eye. Brain Res Dev Brain Res 156, 104–109.
Fuhrmann, S., Stark, M.R., Heller, S., 2003. Expression of Frizzled genes in the developing chick eye. Gene Expr. Patterns 3, 659–662.
Gao, B., Ajima, R., Yang, W., Li, C., Song, H., Anderson, M.J., Liu, R.R., Lewandoski, M. B., Yamaguchi, T.P., Yang, Y., 2018. Coordinated directional outgrowth and pattern formation by integration of Wnt5a and Fgf signaling in planar cell polarity. Development 145 dev163824.
Goodrich, L.V., Strutt, D., 2011. Principles of planar polarity in animal development. Development 138, 1877–1892.
Helmbacher, F., 2020. Fat1 regulates astrocyte maturation and angiogenesis in the retina. bioRxiv, 2020, 2004.2023.057141.
Horne-Badovinac, S., 2017. Fat-like cadherins in cell migration-leading from both the front and the back. Curr. Opin. Cell Biol. 48, 26–32.
Hua, Z.L., Chang, H., Wang, Y., Smallwood, P.M., Nathans, J., 2014. Partial interchangeability of Fz3 and Fz6 in tissue polarity signaling for epithelial orientation and axon growth and guidance. Development 141, 3944–3954.
Hua, Z.L., Smallwood, P.M., Nathans, J., 2013. Frizzled3 controls axonal development in distinct populations of cranial and spinal motor neurons. eLife 2013;2:e01482. doi: 10.7554/eLife.01482.
Jessen, J.R., Solnica-Krezel, L., 2004. Identification and developmental expression pattern of van gogh-like 1, a second zebrafish strabismus homologue. Gene Expression Patterns 4, 339–344.
Krol, A., Henle, S.J., Goodrich, L.V., 2016. Fat3 and Ena/VASP proteins influence the emergence of asymmetric cell morphology in the developing retina. Development 143, 2172–2182.
Lahrouchi, N., George, A., Ratbi, I., Schneider, R., Elalaoui, S.C., Moosa, S., Bharti, S., Sharma, R., Abu-Asab, M., Onojafe, F., 2019. Homozygous frameshift mutations in FAT1 cause a syndrome characterized by colobomatous-microphthalmia, ptosis, nephropathy and syndactyly. Nat. Commun. 10, 1–11.
Leung, L.C., Harris, W.A., Holt, C.E., Piper, M., 2015. NF-protocadherin regulates retinal ganglion cell axon behaviour in the developing visual system. PloS One 10 e0141290.
Lewis, A., Wilson, N., Stearns, G., Johnson, N., Nelson, R., Brockerhoff, S.E., 2011. Celsr3 is required for normal development of GABA circuits in the inner retina. PLoS Genet. 7 e1002239.
Lewis, A.A., Mahoney, J.T., Wilson, N., Brockerhoff, S.E., 2015. Identification of amacrine subtypes that express the atypical cadherin celsr3. Exp. Eye Res. 130, 51–57.
Li, L., Li, H., Wang, L., Wu, S., Lv, L., Tahir, A., Xiao, X., Wong, C.K., Sun, F., Ge, R., 2020. Role of cell polarity and planar cell polarity (PCP) proteins in spermatogenesis. Crit. Rev. Biochem. Mol. Biol. 55, 71–87.
Linser, P., Moscona, A.A., 1981. Carbonic anhydrase C in the neural retina: transition from generalized to glia-specific cell localization during embryonic development. Proc. Natl. Acad. Sci. U.S.A. 78, 7190–7194.
Liu, C., Lin, C., Whitaker, D.T., Bakeri, H., Bulgakov, O.V., Liu, P., Lei, J., Dong, L., Li, T., Swaroop, A., 2013. Prickle1 is expressed in distinct cell populations of the central nervous system and contributes to neuronal morphogenesis. Hum. Mol. Genet. 22, 2234–2246.
Liu, C., Nathans, J., 2008. An essential role for frizzled 5 in mammalian ocular development. Development 135, 3567–3576.
Liu, H., Mohamed, O., Dufort, D., Wallace, V.A., 2003. Characterization of Wnt signaling components and activation of the Wnt canonical pathway in the murine retina. Dev. Dynam. : an official publication of the American Association of Anatomists 227, 323–334.
Liu, X., Zhang, Z., Ribelayga, C.P., 2012. Heterogeneous expression of the core circadian clock proteins among neuronal cell types in mouse retina. PloS One 7 e50602.
Luo, Z., Xu, C., Li, K., Xian, B., Liu, Y., Li, K., Liu, Y., Rong, H., Tang, M., Hu, D., Yang, S., Ye, M., Zhong, X., Ge, J., 2019. Islet1 and Brn3 expression pattern study in human retina and hiPSC-derived retinal organoid. Stem Cell. Int. 2019, 8786396.
Martin-Partido, G., Francisco-Morcillo, J., 2015. The role of Islet-1 in cell specification, differentiation, and maintenance of phenotypes in the vertebrate neural retina. NEURAL REGENERATION RESEARCH 10, 2.
McCabe, K.L., Gunther, E.C., Reh, T.A., 1999. The development of the pattern of retinal ganglion cells in the chick retina: mechanisms that control differentiation. Development 126, 5713–5724.
Mei, X., Westfall, T.A., Zhang, Q., Sheffield, V.C., Bassuk, A.G., Slusarski, D.C., 2014. Functional characterization of Prickle 2 and BBS7 identify overlapping phenotypes yet distinct mechanisms. Dev. Biol. 392, 245–255.
Morino, P., Buchstaller, A., Giger, R., Sonderegger, P., Rager, G., 1996. Differential expression of the mRNAs of the axonal glycoproteins axonin-1 and NgCAM in the developing chick retina. Brain Res Dev Brain Res 91, 252–259.
Nagae, S., Tanoue, T., Takeichi, M., 2007. Temporal and spatial expression profiles of the Fat3 protein, a giant cadherin molecule, during mouse development. Dev. Dynam. : an official publication of the American Association of Anatomists 236, 534–543.
Najarro, E.H., Huang, J., Jacobo, A., Quiruz, L.A., Grillet, N., Cheng, A.G., 2020. Dual regulation of planar polarization by secreted Wnts and Vangl2 in the developing mouse cochlea. Development 147.
Okada, M., Erickson, A., Hendrickson, A., 1994. Light and electron microscopic analysis of synaptic development in Macaca monkey retina as detected by immunocytochemical labeling for the synaptic vesicle protein, SV2. J. Comp. Neurol. 339, 535–558.
Onishi, K., Tian, R., Feng, B., Liu, Y., Wang, J., Li, Y., Zou, Y., 2020. LRRK2 mediates axon development by regulating Frizzled3 phosphorylation and growth cone-growth cone communication. Proc. Natl. Acad. Sci. U.S.A. 117, 18037–18048.
Pavón-Muñoz, T., Bejarano-Escobar, R., Blasco, M., Martín-Partido, G., FranciscoMorcillo, J., 2016. Retinal development in the gilthead seabream Sparus aurata. J. Fish Biol. 88, 492–507.
Prada, C., Puga, J., Perez-Mendez, L., Lopez Ramirez, G., 1991. Spatial and temporal patterns of neurogenesis in the chick retina. Eur. J. Neurosci. 3, 559–569.
Qu, J., Wang, D., Grosskreutz, C.L., 2010. Mechanisms of retinal ganglion cell injury and defense in glaucoma. Exp. Eye Res. 91, 48–53.
Rachel, R.A., Murdoch, J.N., Beermann, F., Copp, A.J., Mason, C.A., 2000. Retinal axon misrouting at the optic chiasm in mice with neural tube closure defects. Genesis 27, 32–47.
Sale, W.S., Besharse, J.C., Piperno, G., 1988. Distribution of acetylated alpha-tubulin in retina and in vitro-assembled microtubules. Cell Motil Cytoskeleton 9, 243–253.
Sanna, P.P., Keyser, K.T., Deerink, T.J., Ellisman, M.H., Karten, H.J., Bloom, F.E., 1992. Distribution and ontogeny of parvalbumin immunoreactivity in the chicken retina. Neuroscience 47, 745–751.
Seigfried, F.A., Cizelsky, W., Pfister, A.S., Dietmann, P., Walther, P., Kühl, M., Kühl, S.J., 2017. Frizzled 3 acts upstream of Alcam during embryonic eye development. Dev. Biol. 426, 69–83.
Senut, M.C., Gulati-Leekha, A., Goldman, D., 2004. An element in the alpha 1-tubulin promoter is necessary for retinal expression during optic nerve regeneration but not after eye injury in the adult zebrafish. J. Neurosci. : the official journal of the Society for Neuroscience 24, 7663–7673.
Shen, N., Qu, Y., Yu, Y., So, K.F., Goffinet, A.M., Vardi, N., Xu, Y., Zhou, L., 2016. Frizzled3 shapes the development of retinal rod bipolar cells. Invest. Ophthalmol. Vis. Sci. 57, 2788–2796.
Singh, J., Mlodzik, M., 2012. Planar cell polarity signaling: coordination of cellular orientation across tissues. Wiley Interdisciplinary Reviews: Dev. Biol. 1, 479–499.
Snow, R.L., Robson, J.A., 1994. Ganglion cell neurogenesis, migration and early differentiation in the chick retina. Neuroscience 58, 399–409.

Song, P., Dudinsky, L., Fogerty, J., Gaivin, R., Perkins, B.D., 2016. Arl13b interacts with Vangl2 to regulate cilia and photoreceptor outer segment length in zebrafish. Invest. Ophthalmol. Vis. Sci. 57, 4517–4526.
Sugiyama, Y., Shelley, E.J., Yoder, B.K., Kozmik, Z., May-Simera, H.L., Beales, P.L., Lovicu, F.J., McAvoy, J.W., 2016. Non-essential role for cilia in coordinating precise alignment of lens fibres. Mech. Dev. 139, 10–17.
Tissir, F., Goffinet, A.M., 2006. Expression of planar cell polarity genes during development of the mouse CNS. Eur. J. Neurosci. 23, 597–607.
Tissir, F., Goffinet, A.M., 2010. Planar cell polarity signaling in neural development. Curr. Opin. Neurobiol. 20, 572–577.
Torban, E., Patenaude, A.M., Leclerc, S., Rakowiecki, S., Gauthier, S., Andelfinger, G., Epstein, D.J., Gros, P., 2008. Genetic interaction between members of the Vangl family causes neural tube defects in mice. Proc. Nat. Acad. Sci. 105 (9), 3449–3454.
Torban, E., Wang, H.J., Patenaude, A.M., Riccomagno, M., Daniels, E., Epstein, D., Gros, P., 2007. Tissue, cellular and sub-cellular localization of the Vangl2 protein during embryonic development: effect of the Lp mutation. Gene Expr. Patterns : GEP 7, 346–354.
Van Raay, T.J., Vetter, M.L., 2004. Wnt/frizzled signaling during vertebrate retinal development. Dev. Neurosci. 26, 352–358.
Wang, X.-J., Zhang, D.-L., Xu, Z.-G., Ma, M.-L., Wang, W.-B., Li, L.-L., Han, X.-L., Huo, Y., Yu, X., Sun, J.-P., 2014. Understanding cadherin EGF LAG seven-pass G-type receptors. J. Neurochem. 131, 699–711.
Wang, Y., Guo, N., Nathans, J., 2006. The role of Frizzled3 and Frizzled 6 in neural tube closure and in the planar polarity of inner-ear sensory hair cells. J. Neurosci. : the official journal of the Society for Neuroscience 26, 2147–2156.
Yu, J.J.S., Maugarny-Calès, A., Pelletier, S., Alexandre, C., Bellaiche, Y., Vincent, J.-P., McGough, I.J., 2020. Frizzled-dependent planar cell polarity without wnt ligands. bioRxiv, 2020, 2005.2023.108977.
Zou, Y., 2020. Breaking symmetry–cell polarity signaling pathways in growth cone guidance and synapse formation. Curr. Opin. Neurobiol. 63, 77–86.